Reducing the Risk of Abrupt Climate Change: Emissions Corridors Preserving the Atlantic Thermohaline Circulation

K. ZICKFELD[1] AND T. BRUCKNER[2]

[1]Potsdam Institute for Climate Impact Research, Potsdam, Germany, and [2]Institute for Energy Engineering, Technical University of Berlin, Berlin, Germany

ABSTRACT

The aim of this paper is to present a modeling framework for deriving emissions corridors that preserve the Atlantic thermohaline circulation (THC). The framework consists of a multi-gas reduced-form climate model coupled to a four-box THC model and allows for the main physical uncertainties (i.e., climate and North Atlantic hydrological sensitivity) to be taken into account. The emissions corridors are calculated along the conceptual and methodological lines of the tolerable windows approach (TWA). The corridor boundaries demarcate emissions limits for the 21st century beyond which either the THC collapses or the mitigation burden becomes intolerable. Accordingly, the corridors represent the maneuvering space for climate policies committed to preserve the THC without endangering future economic growth. Results indicate a large dependence of the width of the emissions corridors on climate and North Atlantic hydrological sensitivity: for low values of climate and/or hydrological sensitivity the upper corridor boundary is far from being transgressed by any of the SRES emissions scenario for the 21st century, while for high values of both quantities even low non-intervention scenarios leave the corridor.

Keywords: climate change, thermohaline circulation, tolerable windows approach, emissions corridors, sensitivity analysis.

1. INTRODUCTION

Potentially unstable features of the climate system have gained increasing scientific and public attention, because they could be the origin of major and rapid disruptions of the human life support systems [1]. A prominent example for this is a conceivable breakdown of the Atlantic thermohaline circulation (THC), i.e., that part of the Atlantic ocean circulation which is driven by density gradients. This circulation transports large amounts of heat northward (in the order of $1 \, \text{PW} = 10^{15} \, \text{W}$), acting as a heating system for north-western Europe and the northern North Atlantic [2]. Paleo-reconstructions [3] and model simulations [4–6] have shown the potential for a THC instability and raised the concern that global climate change may trigger a transition into a circulation state without deep water formation in the Atlantic. Because of the potentially severe consequences for the climate of the North Atlantic region, a collapse of the THC may be considered as a 'dangerous anthropogenic interference with the climate system' that Article 2 of the United Nations Framework Convention on Climate Change (UNFCCC) calls to avoid. The aim of this paper is to present a method for calculating emissions corridors which keep the THC in its present mode of operation, while considering expectations about the socio-economically acceptable pace of emissions reductions efforts. Emissions corridors represent the range of CO_2 emissions that are compatible with normatively defined policy goals or 'guard-rails.' They are calculated on the conceptual basis of the 'tolerable windows approach' (TWA or 'guard-rail approach' [7, 8]). The TWA differs fundamentally from conventional integrated assessment approaches, such as cost-benefit [9–11] and cost-effectiveness analysis [12], as it does not seek to identify a single 'optimal' emissions path, but the full bundle of paths admissible under the pre-defined guard-rails [13, 14]. The first attempt to consider irreversible changes in the THC in the framework of the TWA was made in [15]. This study used the stability diagram of the THC determined in [5] as a static constraint on emissions trajectories. This was a valid first attempt, but implied some drastic simplifications as argued in [15]. The modeling framework presented here includes a dynamic THC model and may be understood as an advancement of the work reported in [15].

2. METHODOLOGY AND MODEL COMPONENTS

The analytical tool employed for this study consists of a dynamic box model of the Atlantic thermohaline circulation coupled to a multi-gas reduced-form climate model. The guard-rail approach outlined in Section 1 is implemented as a specially formulated control problem. Section 2.1 sketches the mathematical background and describes the algorithm for calculating emissions corridors. Section 2.2 presents the reduced-form model of the THC. Section 2.3 describes how scenarios of global mean temperature are translated into scenarios of basin-wide climate variables that are required to drive the THC model. The reduced-form climate model providing the global mean temperature scenarios is presented in Section 2.4. A short description of the dynamic behavior of the coupled THC-climate model is given in Section 2.5. Section 2.6 specifies the climate impact guard-rails and the socio-economically motivated constraints on the emissions behavior that we have used in this study.

2.1. Calculation of Emissions Corridors

In mathematical terms, the derivation of emissions corridors may be formulated as a dynamic control problem. The time evolution of the system is described by the state vector $\mathbf{x}(t)$, and is subject to the set of differential equations:

$$\dot{\mathbf{x}}(t) = \mathbf{f}(\mathbf{x}(t), \mathbf{u}(t), t), \tag{1}$$

with initial conditions $\mathbf{x}(t=0) = \mathbf{x}_0$ and restricted controls $\mathbf{u}(t) \in \mathcal{U}$, where $\mathcal{U}$ is the set of all possible control measures. Further, the system is required to remain within boundaries specified by guard-rails of the form:

$$\mathbf{h}(\mathbf{x}(t), \mathbf{u}(t), t) \leq \mathbf{0}. \tag{2}$$

In our specific analysis, the state vector $\mathbf{x}(t)$ includes variables like global mean temperature, concentrations of all major greenhouse gases, and the Atlantic thermohaline circulation rate. The control vector $\mathbf{u}(t)$ comprises the level of energy-related CO_2 emissions. The guard-rails constrain the intensity of the THC to remain above a certain level and express expectations about the socio-economically acceptable pace of emissions reductions (cf. Section 2.6).

The TWA seeks to identify the complete bundle of control paths $\mathbf{u}(\cdot)$ and corresponding state trajectories $\mathbf{x}(\cdot)$ which are governed by the set of differential equations Eq. (1), with initial conditions $\mathbf{x}_0$, and subject to the constraints described by Eq. (2). A suitable mathematical framework for the description of the set-valued solution to this problem has proven to be the theory of differential inclusions [16]. Although determining the full solution (i.e., the admissible bundle) is not feasible at the current state of this theory, it is possible to derive interesting properties of this bundle. For example, a combination of concepts from the fields of differential inclusions and control theory [17] allows for the determination of the outer boundaries of the admissible control space $\mathbf{u}(\cdot)$ [18, 19]. The projection of the area between these boundaries onto a subspace spanned by time and CO_2 emissions is what is referred to as an 'emissions corridor' (cf. [20]). This procedure, however, is associated with loss of information about the inner structure of the corridor. Indeed, the resulting corridors do not contain information about the dynamics of the system, i.e., which points within the corridor are connected by admissible paths. This has the important consequence that the corridors impose a necessary but not a sufficient condition on the admissibility of a particular emissions path: all paths which are compatible with the guard-rails lie within the corridor, but not every path which lies within the corridor is necessarily admissible. A concept for constructing sufficient corridors is outlined in [21].

The concrete algorithm for the computation of the upper (lower) boundary of an emissions corridor consists in successively maximizing (minimizing) CO_2 emissions for fixed points in time t_i. The entire upper (lower) boundary is then constructed by the maxima (minima) of such emissions paths (cf. [18]). In the experiments presented in this paper, the upper and lower boundaries are calculated for the period 2000–2100 in time steps of 5 years. The time horizon of the optimizations is set to 2400 in order to account for the inertia of the climate system and to ensure that an emissions path observing the guard-rails in the 21st century does not lead to a violation in the centuries to follow. For the numerical solutions of the optimization problems, the GAMS package (General Algebraic Modeling System; [22]) is employed. Figure 4 illustrates the algorithm for the calculation of emissions corridors by displaying paths maximizing emissions in the years 2020, 2060, and 2100.

2.2. Reduced-Form Model of the Atlantic Thermohaline Circulation

Because of the high computational costs of the optimization procedure employed for the calculation of emissions corridors, conventional models representing the THC (general circulation models as well as models of intermediate complexity) are too costly to be incorporated in the framework of the TWA. We thus developed a computationally efficient reduced-form dynamic model of the THC, which, although highly simplified compared to the comprehensive models, reliably reproduces the salient features of their results.

The model is an inter-hemispheric extension of the classic Stommel model [23] – a conceptual model that has been successfully applied for the investigation of bifurcations and the stability of the Atlantic thermohaline circulation [24, 25]. While in these studies the steady-state solutions of the model were investigated, we reformulate the model in dynamical terms and compute its time-dependent behavior. In this aspect, our approach is similar to that followed by Schneider and Thompson [26] who applied a two-box model called the 'Simple Climate Demonstrator.'
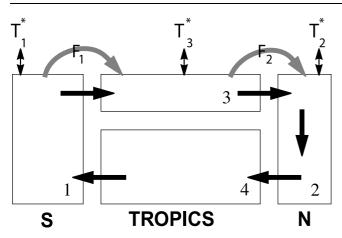
Fig. 1. Schematic of the four-box model of the Atlantic thermohaline circulation. The temperatures of boxes 1, 2, and 3 are relaxed toward the values T_1^*, and T_2^*, and T_3^*, respectively. The salinities are forced by the freshwater fluxes F_1 and F_2. The meridional flow (black arrows) is proportional to the density gradient between boxes 1 and 2.

Our model configuration is shown in Figure 1. It consists of four well-mixed basins, representing the southern, tropical, northern, and deep Atlantic, respectively. Neighbouring boxes are connected to allow for a continuous, closed-loop circulation. The surface boxes are linked to the overlying atmosphere through fluxes of heat and freshwater. Assuming that the water in the northern basin is denser than the water in the southern basin, a pressure-driven circulation develops with northward flow near the surface and southward flow at depth. This picture is consistent with the accepted notion of the Atlantic THC as a cross hemispheric system driven by density gradients between the northern and the southern Hemispheres [24, 27].

In this four-box model, the meridional volume transport m (or overturning) is proportional to the density difference $\rho_2 - \rho_1$ between boxes 1 and 2:

$$m = \frac{k(\rho_2 - \rho_1)}{\rho_0}$$
$$= k[\beta(S_2 - S_1) - \alpha(T_2 - T_1)], \qquad (3)$$

where $S_2 - S_1$ and $T_2 - T_1$ are the north-south salinity and temperature gradients, respectively. k is a hydraulic constant linking volume transport m to the density difference, ρ is a reference density, α and β are the thermal and haline expansion coefficients, respectively.

The temperatures and salinities of the four boxes adjust to the oceanic transport of heat and freshwater. Further, temperatures and salinities of the surface boxes are forced by the overlying atmosphere through fluxes of heat and freshwater. The surface heat fluxes are described by a Newtonian restoring law of the form $Q \propto (T^* - T)$, where T^* denotes the relaxation temperature. Salinity forcing consists of fixed atmospheric vapour transports between the upper boxes. This leads to the following set of ordinary differential equations for temperatures T_i and salinities S_i for each of the four boxes:

$$\dot{T}_1 = \frac{m}{V_1}(T_4 - T_1) + \lambda_1(T_1^* - T_1) \qquad (4)$$

$$\dot{T}_2 = \frac{m}{V_2}(T_3 - T_2) + \lambda_2(T_2^* - T_2) \qquad (5)$$

$$\dot{T}_3 = \frac{m}{V_3}(T_1 - T_3) + \lambda_3(T_3^* - T_3) \qquad (6)$$

$$\dot{T}_4 = \frac{m}{V_4}(T_2 - T_4) \qquad (7)$$

$$\dot{S}_1 = \frac{m}{V_1}(S_4 - S_1) + \frac{S_0 F_1}{V_1} \qquad (8)$$

$$\dot{S}_2 = \frac{m}{V_2}(S_3 - S_2) - \frac{S_0 F_2}{V_2} \qquad (9)$$

$$\dot{S}_3 = \frac{m}{V_3}(S_1 - S_3) - \frac{S_0(F_1 - F_2)}{V_3} \qquad (10)$$

$$\dot{S}_4 = \frac{m}{V_4}(S_2 - S_4). \qquad (11)$$

Here V_i are box volumes, λ_i thermal coupling constants, and T_i^* the temperatures the southern, northern and tropical boxes are relaxed towards. F_1 and F_2 are the freshwater fluxes (multiplied by a reference salinity, S_0, for conversion to a salt flux) into the tropical and northern Atlantic, respectively.

The steady-state solutions for the T_i and S_i are obtained analytically from Eqs. (4)–(11) and can be expressed as functions of the parameters only (cf. [28]). Substituting these expressions into Eq. (3) leads to a non-linear relationship between the volume transport m and the Atlantic freshwater forcing F_1, implying the existence of a threshold value in the latter beyond which the circulation shuts down. Under equilibrium, F_2 plays only a minor role, as it does not affect the volume transport m. In the transient case, however, it is very effective in determining changes in m. Indeed, an extreme freshwater forcing F_2 may trigger a complete shutdown of the circulation (for an in-depth discussion of the role of the freshwater fluxes F_i and the stability properties of the four-box model cf. [24]). Note that the steady-state solutions for the T_i, the S_i and m serve as initial conditions for the computation of the time-dependent trajectories of the box model.

In order to tune the box model to present-day climate conditions we fitted the unknown parameters $T_{i,0}^*$, $F_{i,0}$ (which denote the present-day values for the T_i^* and F_i), k and λ_i, to results obtained with the climate model CLIMBER-2 [29, 30]. This coupled model of intermediate complexity has proven to successfully describe crucial elements of the climate system, including the THC. We have chosen CLIMBER-2 as reference because of its computational efficiency which allows one to perform a number of simulations within a manageable time-frame. Notwithstanding, any other coupled climate model could be used. The fitting procedure and the resulting parameter values are described in detail in [28, 31].

2.3. Linking the THC Box Model to a Globally Aggregated Climate Model

Our intention is to use the box model to diagnose the transient response of the Atlantic THC to scenarios of global mean temperature change. In order to drive the model, global mean temperature has thus to be appropriately down-scaled into basin-wide patterns of changes in restoring temperatures ΔT_i^* and freshwater fluxes ΔF_i. A common method for the efficient construction of regionally explicit climate change projections is the so-called scaled scenario approach [32, 33]. It describes future climate change by scaling spatial patterns of climate anomalies by the respective global mean temperature change ΔT^{GL}. Following this approach, changes in restoring temperatures ΔT_i^* evolve according to:

$$\Delta T_i^*(t) = p_i \Delta T^{GL}(t), \quad i \in \{1, 2, 3\}, \tag{12}$$

with constant coefficients p_i. For determining the time evolution of the freshwater forcing, we take advantage of the fact that in CLIMBER-2 (as well as in other models) changes in the meridional freshwater transports are approximately proportional to the temperature change in the northern and southern Hemisphere, i.e. ΔT^{NH} and ΔT^{SH}, respectively (cf. [6]):

$$\Delta F_1(t) = h_1 \Delta T^{SH}(t) = h_1 p^{SH} \Delta T^{GL}(t), \tag{13}$$

$$\Delta F_2(t) = h_2 \Delta T^{NH}(t) = h_2 p^{NH} \Delta T^{GL}(t). \tag{14}$$

The proportionality constants p_i and h_i, which are derived from greenhouse gas simulations with the CLIMBER-2 model (cf. [28]), are shown in Table 1. h_2 considers changes in the freshwater flux into the Atlantic north of 50°N and is in the following referred to as 'North Atlantic hydrological sensitivity.' It must be noted that the value for h_2 diagnosed in CLIMBER-2 is $0.013\,\text{Sv}/°\text{C}$, i.e., lower then the one

Table 1. Standard model parameters. Note that 1 Sv corresponds to $10^6\,\text{m}^3/\text{s}$.

Model parameters	
Regional temperature constants	
p_1	0.86
p_2	1.07
p_3	0.79
p^{SH}	0.93
p^{NH}	1.07
Hydrological sensitivities	
h_1	$-0.005\,\text{Sv}°\text{C}^{-1}$
h_2	$0.03\,\text{Sv}°\text{C}^{-1}$
Climate sensitivity	
$T_{2 \times CO_2}$	$2.5\,°\text{C}$
Guard-rails	
m_{min}	$10\,\text{Sv}$
r	$0.015\,\text{yr}^{-1}$
t_{trans}	$20\,\text{yrs}$

indicated in Table 1. The actual choice is motivated by the fact that the North Atlantic hydrological sensitivity derived from CLIMBER-2 is low compared with the values diagnosed in other models. As standard value we thus adopt a value which lies in the middle of the plausible range of 0.01–$0.05\,\text{Sv}/°\text{C}$ (cf. [6]).

The above formulation of temperature and freshwater forcing allows for a large flexibility in the consideration of uncertainties about the amount and regional distribution of global warming and associated changes in the hydrological cycle, which are among the main uncertain factors in predicting the response of the THC to climate change scenarios. Indeed, quantities which are 'diagnostic' in conventional climate models are represented here as parameters and can easily be varied.

2.4. Climate Model

For projections of global mean temperature, we use the ICLIPS multi-gas climate model [34], which is a computationally efficient, globally aggregated model capable of mimicking the response of sophisticated carbon-cycle and atmosphere-ocean general circulation models. The model translates anthropogenic emissions of CO_2, CH_4, N_2O, halocarbons, SF_6, and SO_2 into time-dependent paths for concentrations, radiative forcing and global mean temperature.

The core component of the ICLIPS climate model is a differential analog to a non-linear impulse response function (IRF) model of the coupled carbon-cycle-plus-climate system [35]. Non-linear here means that the IRF model analog includes non-linear physical processes, such as solubility of additional CO_2 in ocean surface waters, response of primary productivity of land vegetation and radiative greenhouse forcing to rising CO_2 concentrations. The inclusion of these processes extends the range of applicability of the IRF model, which would otherwise be limited to concentrations less than twice the preindustrial value [36].

For the modeling of the atmospheric chemistry and radiative forcing of major non-CO_2 greenhouse gases (CH_4, N_2O, halocarbons, SF_6, tropospheric and stratospheric O_3, and stratospheric water vapour) and aerosols (originating from SO_2 and biomass burning) various components of the MAGICC model [37] have been adopted. These components are very similar to the 'simple models' used by the IPCC for scenario analyses reported in its Second Assessment Report (SAR [38, 39]).

The model as presented in [34] is extended for the scope of this paper to allow for the consideration of different climate sensitivities. This is achieved by relating the temperature IRF model to a box-diffusion model analog. Figure 2 displays the response of the climate model to emissions following business-as-usual scenario IS92a [40]. For comparison, the projections presented in the SAR for different climate sensitivities [38] are also shown. The climate model agrees fairly well in its response with the SAR projections.
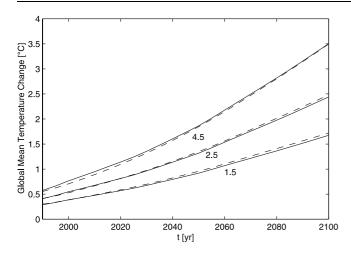
Fig. 2. Temperature projections for different values of the climate sensitivity $T_{2 \times CO_2}$ [°C] following emissions scenario IS92a. The dashed lines are results obtained with the ICLIPS climate model, the solid lines those given in the IPCC SAR [38].

Fig. 3. Stability diagram of the THC in $(T, \dot{T})$ phase space as calculated with the four-box model for different assumptions about the North Atlantic hydrological sensitivity h_2 [Sv/°C]. The stable (unstable) domains are located to the left (right) of the respective curves. For comparison we show the stability curve derived from [5] (labeled 'SS').

2.5. Time-Dependent Response of the Coupled THC-Climate Model

Although comparatively simple, the coupled THC-climate model is able to reproduce the key dynamic features of complex climate models. In response to low CO_2 emissions scenarios, for example, the circulation is weakened and, as soon as concentrations are stabilized, recovers. This agrees with the behavior of comprehensive climate models found, e.g., in [41, 42]. In the case of high emissions scenarios, or assuming high values for the North Atlantic hydrological sensitivity, the circulation shuts down indicating the existence of a threshold value in the freshwater forcing beyond which the circulation cannot be sustained. The latter is similar to the behavior discussed in [4, 6, 42]. Further, we found the response of the overturning in our box model to be sensitive to the rate of temperature increase as described in [5]. An extensive discussion of the model behavior as compared to that of comprehensive climate models is given in [28].

Figure 3 shows the stability diagram of the THC as simulated in the box model for different assumptions about the North Atlantic hydrological sensitivity. It displays some of the key dynamic features of the THC: for a given rate of temperature change, the higher the hydrological sensitivity, the lower the amount of temperature increase that the THC can sustain without collapsing. Also, Figure 3 clearly shows the sensitivity of the THC on the rate of climate change.

2.6. Specification of Guard-Rails

In specifying the guard-rail compatible with the goal of preserving the THC we take advantage of the fact that this system has a well-defined threshold beyond which the circulation shuts down. It can be shown analytically that in
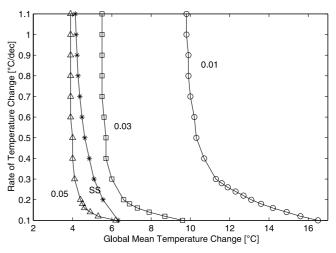
equilibrium the critical flow (i.e., the flow strength beyond which the circulation cannot be sustained and inevitably collapses) corresponds to half the equilibrium overturning [24] and is given as 11.4 Sv in our four-box model (cf. Table 2 in [28]). In the transient case, this picture changes slightly since, as discussed in Section 2.5, the critical threshold is dependent upon the rate of climate change (cf. Fig. 3). We account for this transient effect and specify the minimum admissible overturning m_{min} as 10 Sv. The guard-rail constraining the THC is then given by:

$$m(t) \geq m_{min} = 10 \, \text{Sv} \; \forall t. \tag{15}$$

The expectations about the socio-economically acceptable pace of emissions reductions efforts are expressed by two conditions, which are adopted from [21]. The first specifies the maximum admissible rate of emissions reductions r:

$$g(t) \geq -r \; \forall t \; \text{with} \; g(t) = \dot{E}(t)/E(t), \tag{16}$$

where $E(t)$ denotes industrial CO_2 emissions. The second condition addresses socio-economic inertia by imposing a smoothness constraint on the transition to a decarbonizing economy. This is achieved by requiring a minimum time span t_{trans} for the transition from a regime where emissions increase with a maximum growth rate g_0 to a regime where emissions decrease with the maximum reduction rate r. Further, we introduce a third condition which is mainly technically motivated and concerns the direction of the emissions growth rate g: we require that g decreases monotonously in time, with a maximum emissions growth rate g_0 in the year 2005. As pointed out in [21], this constraint is rather strong as it excludes emissions trajectories where the emissions growth rate itself grows

after 2005. This would be the case, e.g., for emissions scenarios which assume a switch to coal after the exploitation of the oil and gas reserves, as is the case in some of the SRES emissions scenarios [43]. We summarize the last two conditions in a single inequality:

$$-\frac{g_0 + r}{t_{trans}} \leq \dot{g}(t) \leq 0 \ \forall t. \tag{17}$$

For the corridor calculations presented in the following section we assumed a maximum admissible rate of global emissions reductions r of 1.5% per year and a minimum tolerable transition time towards a decarbonizing economy t_{trans} of 20 years.

3. RESULTS

In this section we present emissions corridors compatible with the goal of preserving the THC. First we show the emissions corridor for standard model settings (cf. Table 1) and then discuss the results of a sensitivity analysis with respect to the main uncertain parameters in predicting the THC, i.e., climate and North Atlantic hydrological sensitivity [44]. In all corridor computations, CO_2 emissions from land-use change and emissions of non-CO_2 greenhouse gases are assumed to follow the average of the four SRES marker scenarios (i.e., the average of A1, A2, B1, B2, [43]) until 2100, and then hold constant. SO_2 emissions are linked to industrial CO_2 emissions (i.e., the control variable) assuming a globally averaged desulfurization rate of 1.5% per year.

The corridor for standard parameter settings is displayed in Figure 4, along with selected emissions paths to illustrate

its internal structure. The corridor boundaries demarcate emissions limits beyond which either the THC collapses or the socio-economic guard-rails are violated. It should be reemphasized that emissions corridors impose only a necessary condition on the admissibility of a particular emissions path, implying that not every single path within the corridor is necessarily admissible. For example, the upper boundary of the corridor can be reached in 2060 only if emissions remain far inside the corridor for several decades in the first half of the 21st century.

For purposes of reference, Figure 4 also displays low and high CO_2 emission scenarios (SRES scenario B1 and A2, [43]). We find that for standard parameter values the emissions corridor is wider than the range spanned by the SRES emissions scenarios B1 and A2. This result might suggest that no immediate mitigation effort is necessary in order to preserve the THC. In the following, however, we show that this result is very sensitive to the specific assumptions concerning climate and hydrological sensitivity. In terms of CO_2 concentrations and global mean temperature change, the imposed guard-rails imply a maximum of approximately 1300 ppm reached during the 22nd century followed by a slight decline thereafter and a stabilization at around 5.5 °C, respectively (not shown).

Figure 5 displays emissions corridors for different values of the climate sensitivity $T_{2 \times CO_2}$. The latter parameter is varied in the range from 1.5 to 4.5 °C (with all other parameters at their standard values), which is the uncertainty range indicated by the IPCC [45]. Our findings indicate a very strong dependence of the width of the emissions corridor on climate sensitivity. This sensitivity affects only the position of the upper corridor boundary, as the lower one is solely determined by the maximum emissions reduction rate r and thus is the same for all values of climate
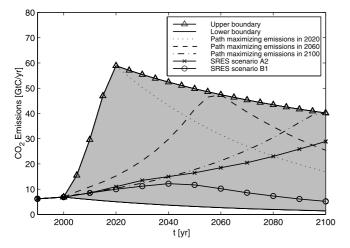

Fig. 4. Emissions corridor – the shaded area between upper and lower boundaries – for standard parameter settings (cf. Table 1). For an illustration of its internal structure we show paths maximizing CO_2 emissions in 2020, 2060, and 2100. For reference we also display representative low and high emissions scenarios (SRES marker scenarios B1 and A2, respectively).
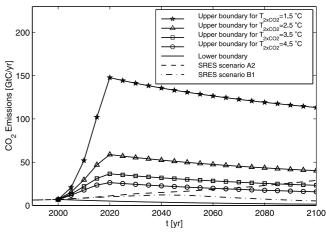

Fig. 5. Emissions corridors for different values of climate sensitivity $T_{2 \times CO_2}$. The lower corridor boundary is the same for all values of $T_{2 \times CO_2}$, as it is solely determined by the maximum emissions reduction rate r.

sensitivity. For a value of 1.5 °C the upper corridor boundary is far from being touched by the emissions projected for the 21st century by the SRES emissions scenarios. For a climate sensitivity of 2.5 °C the upper boundary is still out of reach, but the width of the corridor is considerably reduced (by approximately 60%). For climate sensitivities of 3.5 and 4.5 °C the corridors shrink further, and the high reference emissions scenario (SRES marker scenario A2) crosses the upper corridor boundaries in the second half of the 21st century. It should be emphasized that a transgression of the corridor boundaries does not imply an immediate collapse of the THC: because of the inertia of the ocean, the actual event occurs centuries after it is triggered. Once the corridor boundaries are transgressed, however, a collapse of the THC is inevitable.

In our model two mechanisms contribute to the reduction of the corridor with increasing climate sensitivity: the differential warming between the southern and the northern boxes (compare the values for p_1 and p_2 in Table 1) and the enhanced freshwater transport towards the northern latitudes, which increases with growing global mean temperature (cf. Eq. (14)). Both act to reduce the meridional density gradient which drives the THC and thus weaken the latter.

In further experiments we computed emissions corridors for different values of the North Atlantic hydrological sensitivity h_2, which is one of the main uncertainties faced when predicting the fate of the THC. The reason is that estimates of evaporation and precipitation changes over the North Atlantic differ significantly between models, as well as estimates of freshwater runoff from the Greenland ice sheet and other melting glaciers in the North Atlantic catchment. Here we assume an uncertainty range for h_2 of 0.01–0.05 Sv/°C (for a justification cf. [6]). The resulting emissions corridors are shown in Figure 6. As for climate

sensitivity, the size of the emissions corridors largely depends on the specific parameter choice: for low values of h_2 the corridor is much larger than the range spanned by the SRES emissions scenarios, while for high values SRES emissions scenario A2 transgresses the upper corridor boundary in the second half of the 21st century. This strong sensitivity of the THC on the value of the North Atlantic hydrological sensitivity h_2 was already evident in Figure 3: the higher h_2, the lower the temperature increase and thus the CO_2 load of the atmosphere that can be sustained if the THC is to be kept within its stable domain.

So far we have restricted our discussion to single parameter sensitivity analyses, whereby we varied one parameter, while keeping all others at their standard values. In the following we present emissions corridors for the 'best case,' 'best guess,' and 'worst case' combinations of climate and North Atlantic hydrological sensitivities. Our analysis is based upon the uncertainty range for climate sensitivity given by the IPCC, i.e., 1.5 to 4.5 °C [45]. It must be noted that recent estimates exist, where the uncertainty range for climate sensitivity is extended considerably towards higher values (e.g., [46]). For the North Atlantic hydrological sensitivity we rely on the range of 0.01 to 0.05 Sv/°C given in [6]. The 'best case' and 'worst case' refer to the combinations $T_{2 \times CO_2} = 1.5$ °C, $h_2 = 0.02$ Sv/°C,[1] and $T_{2 \times CO_2} = 4.5$ °C, $h_2 = 0.05$ Sv/°C, respectively. As 'best guess' we take the standard setting of our model, i.e., $T_{2 \times CO_2} = 2.5$ °C, $h_2 = 0.03$ Sv/°C.

The results are displayed in Figure 7. For the 'best case' the upper corridor boundary is far from any of the SRES being reached by emissions scenarios for the 21st century. As discussed previously, for the 'best guess' case the corridor is still larger than the range spanned by the SRES emissions scenarios. For the 'worst case' combination of model parameters, however, the corridor almost vanishes, such that even the low emissions scenario B1 leaves the corridor in the first half of the 21st century. The shaded areas in Figure 7 may be interpreted as likelihood domains for a collapse of the THC: the darker the shading of the area that any given emissions scenario enters, the higher the probability that a complete and irreversible breakdown of the THC is triggered.

One remaining question concerns the sensitivity of the emissions corridors to the socio-economically motivated guard-rails expressed by the parameters r and t_{trans}. We computed the emissions corridors for a few values of these quantities. Our results indicate that the sensitivity of the corridors to the maximum emissions reduction rate r is significant throughout the 21st century: lowering (increasing) r by 0.5% leads to a reduction (increase) of the corridor area by approximately 20%. The transition time t_{trans}, on the
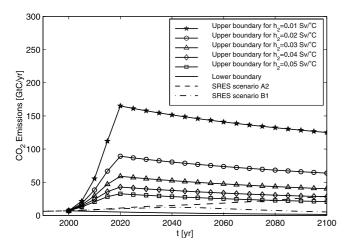

Fig. 6. Emissions corridors for different values of the North Atlantic hydrological sensitivity h_2 (with all other parameters at their standard values).

---

[1]The corridor for the parameter combination $T_{2 \times CO_2} = 1.5$ °C, $h_2 = 0.01$ Sv/°C cannot be calculated since the allowable emissions exceed the domain of applicability of the coupled-carbon-cycle-plus-climate-model.
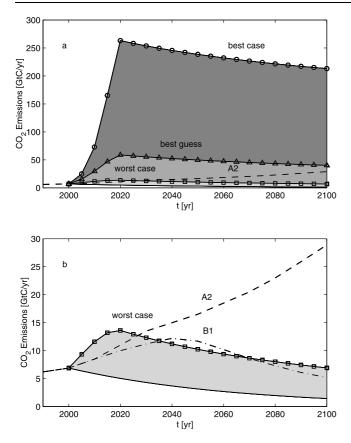
Fig. 7. (a) Emissions corridors for the 'best case,' 'best guess,' and 'worst case' combinations of model parameter values. The shaded areas between the corridors indicate likelihood domains for a shutdown of the THC: the darker the shading, the higher the probability that any given emissions paths entering that domain triggers a breakdown of the THC. For reference we show SRES marker emissions scenario A2. (b) Zoom into the 'worst case' corridor shown in (a).

The ability to consider climate related uncertainties in our model is crucial since projections of changes in the THC vary widely among comprehensive climate models (cf. Fig. 9.21 in [45]). This discrepancy is attributed mainly to differences in the simulation of surface fluxes of heat and freshwater and to a diversity of schemes for describing sub-grid scale mixing processes in the ocean [45]. The uncertainty in ocean surface forcing can be accounted for in our framework by varying the values of climate and hydrological sensitivity and of the regional temperature constants (cf. Table 1). Since mixing is not modeled explicitly in the reduced-form THC model, uncertainties in this factor can only be captured by fitting the four-box model to coupled climate models other than our reference model CLIMBER-2 and then performing a sensitivity analysis with respect to the resulting parameter sets. This step was not part of the present work. An in-depth investigation into the behavior of the reduced-form THC model [28] nevertheless indicates that the sensitivity analysis conducted in this study allows one to capture the range of THC responses exhibited by comprehensive climate models. Whether this range comprises the response of the 'real' ocean is uncertain. The reason is that comprehensive climate models may be biased since their representation of some physical processes is insufficient. One example is the physics involved in the sinking of the high density water in the North Atlantic, which is essential in driving the THC. This ulterior uncertainty should be taken into account when interpreting the results presented in this paper.

One shortcoming of our framework so far is the rudimentary representation of the socio-economic sphere. The inclusion of an integrated energy-economy model is underway, which will allow one to specify guard-rails in domains that are more meaningful to policymakers, such as greenhouse gas mitigation costs.

Results obtained within our modeling framework indicate that for the 'best guess' choice of model parameters, the CO_2 emissions corridor is larger than the range spanned by the SRES emissions scenarios for the 21st century. We tested the robustness of this finding by performing a sensitivity analysis with respect to the main uncertain physical quantities in projecting the fate of the THC, i.e., climate and North Atlantic hydrological sensitivities. We found that the width of the emissions corridor is largely dependent upon the specific parameter choice: for low values of climate and/or hydrological sensitivity the upper corridor boundary is far from being reached by any of the SRES emissions scenarios, while for high values of both parameters the corridor area is considerably tightened. These model results indicate that, given the amount of greenhouse gases already in the atmosphere, and the inertia of the climate system, the maneuvering space for climate policies committed to the precautionary principle may well be tight. Indeed, already the low non-intervention emissions scenario B1 departs the 'worst case' corridor in the first half of the 21st century. The

other hand, is found to affect the shape of the emissions corridors mainly in the first decades of the century (cf. [21]). Another uncertainty concerns emissions of non-CO_2 greenhouse gases, which were so far assumed to follow the average of the four SRES marker scenarios. Assuming lower emissions (for example, non-CO_2 greenhouse gases following SRES scenario B1) increases the leeway for preserving the Atlantic THC significantly.

4. CONCLUSIONS AND OUTLOOK

In this paper we presented a modeling framework well suited for identifying the leeway for climate policies committed to the preservation of the Atlantic thermohaline circulation without endangering future economic growth. One strength of this framework is that it allows for comprehensive sensitivity analyses with respect to main physical and socio-economic parameters.

leeway is enlarged in our model if mitigation options for non-CO_2 greenhouse gases are considered or expectations about the socio-economically acceptable pace of CO_2 emissions reduction are relaxed, i.e., the minimum admissible transition time t_{trans} is decreased and the maximum admissible emissions reduction rate r is increased.

REFERENCES

1. Smith, J., Schellnhuber, H.-J. and Mirza, M.Q.: Lines of Evidence for Vulnerability to Climate Change: A Synthesis. In: J.J. McCarthy, O.F. Canziani, N.A. Leary, D.J. Dokken, K.S. White (eds.): *Climate Change 2001: Impacts, Adaptation and Vulnerability – Contribution of Working Group II to the Third Assessment Report of the IPCC*. Cambridge University Press, Cambridge, 2001, pp. 914–967.
2. Macdonald, A.M. and Wunsch, C.: An Estimate of Global Ocean Circulation and Heat Fluxes. *Nature* 382 (1996), pp. 436–439.
3. Dansgaard, W., Johnsen, S.J., Clausen, H.B., Dahl-Jensen, N.S., Gundestrup, N.S., Hammer, C.U., Hvidberg, C.S., Steffensen, J.P., Sveinbjoernsdottir, A.E., Jouzel, J. and Bond, G.: Evidence for General Instability of Past Climate from a 250-kyr Ice-Core Record. *Nature* 364 (1993), pp. 218–220.
4. Manabe, S. and Stouffer, R.J.: Century-Scale Effects of Increased Atmospheric CO_2 on the Ocean-Atmosphere System. *Nature* 364 (1993), pp. 215–218.
5. Stocker, T.F. and Schmittner, A.: Influence of CO_2 Emission Rates on the Stability of the Thermohaline Circulation. *Nature* 388 (1997), pp. 862–865.
6. Rahmstorf, S. and Ganopolski, A.: Long-Term Global Warming Scenarios Computed With an Efficient Coupled Climate Model. *Clim. Change* 43 (1999), pp. 353–367.
7. Petschel-Held, G., Schellnhuber, H.-J., Bruckner, T., Tóth, F.L. and Hasselmann, K.: The Tolerable Windows Approach: Theoretical and Methodological Foundations. *Clim. Change* 41 (1999), pp. 303–331.
8. Bruckner, T., Petschel-Held, G., Tóth, F.L., Füssel, H.M., Helm, C., Leimbach, M. and Schellnhuber, H.J.: Climate Change Decision Support and the Tolerable Windows Approach. *Environ. Model. Assess.* 4 (1999), pp. 217–234.
9. Nordhaus, W.D.: *Managing the Global Commons: The Economics of Climate Change*. MIT Press, Cambridge, MA, 1994.
10. Keller, K., Tan, K., Morel, F.M.M. and Bradford, D.F.: Preserving the Ocean Circulation: Implications for Climate Policy. *Clim. Change* 47 (2000), pp. 17–43.
11. Mastrandrea, M.D. and Schneider, S.H.: Integrated Assessment of Abrupt Climatic Changes. *Clim. Policy* 1 (2001), pp. 433–449.
12. Manne, A.S., Mendelsohn, R. and Richels, R.G.: MERGE: A Model for Evaluating Regional and Global Effects of Greenhouse Gas Reduction Policies. *Energy Policy* 23 (1995), pp. 17–34.
13. Tóth, F.L., Bruckner, T., Füssel, H.-M., Leimbach, M. and Petschel-Held, G.: Integrated Assessment of Long-Term Climate Policies: Part 1 – Model Presentation. *Clim. Change* 56 (2003), pp. 37–56.
14. Tóth, F.L., Bruckner, T., Füssel, H.-M., Leimbach, M. and Petschel-Held, G.: Integrated Assessment of Long-Term Climate Policies: Part 2 – Model Results and Uncertainty Analysis. *Clim. Change* 56 (2003), pp. 57–72.
15. Tóth, F.L., Petschel-Held, G. and Bruckner, T.: Kyoto and the Long-Term Climate Stabilization. In: *Proceedings of the OECD Workshop on Economic Modeling of Climate Change*, Paris, September, 17–18, 1998.
16. Aubin, J.P.: *Viability Theory*. Birkhäuser, Basel, 1991.
17. Papageorgiou, M.: *Optimierung*. Oldenbourg, München, 1991.
18. Leimbach, M. and Bruckner, T.: Influence of Economic Constraints on the Shape of Emission Corridors. *Comput. Eco.* 18 (2001), pp. 173–191.
19. Bruckner, T., Petschel-Held, G., Leimbach, M. and Tóth, F.L.: Methodological Aspects of the Tolerable Windows Approach. *Clim. Change* 56 (2003), pp. 73–89.
20. Alcamo, J. and Kreileman, E.: Emission Scenarios and Global Climate Protection. *Glob. Environ. Change* 6 (1996), pp. 305–334.
21. Kriegler, E. and Bruckner, T.: Sensitivity Analysis of Emissions Corridors for the 21st Century. *Clim. Change* (2003), submitted.
22. Brooke, A., Kendrick, D. and Meeraus, A.: *GAMS: A User's Guide*, Release 2.25. Scientific Press, San Francisco, USA, 1992.
23. Stommel, H.: Thermohaline Convection With Two Stable Regimes of Flow. *Tellus* 13 (1961), pp. 224–241.
24. Rahmstorf, S.: On the Freshwater Forcing and Transport of the Atlantic Thermohaline Circulation. *Clim. Dyn.* 12 (1996), pp. 799–811.
25. Scott, J.R., Marotzke, J. and Stone, P.H.: Inter-Hemispheric Thermohaline Circulation in a Coupled Box Model. *J. Phys. Oceanogr.* 29 (1999), pp. 351–365.
26. Schneider, S.H. and Thompson, S.L.: Simple Climate Model Used in Economic Studies of Global Change. In: S.J. DeCanio, R.B. Howarth, A.H. Sanstad, S.H. Schneider, S.L. Thompson (eds.): *New Directions in the Economics and Integrated Assessment of Global Climate Change*. Pew Center on Global Climate Change, Arlington, VA, 2000, pp. 59–80.
27. Thorpe, R.B., Gregory, J.M., Johns, T.C., Wood, R.A. and Mitchell, J.F.B.: Mechanisms Determining the Atlantic Thermohaline Circulation Response to Greenhouse Gas Forcing in a Non-Flux-Adjusted Coupled Climate Model. *J. Clim.* 14 (2001), pp. 3102–3116.
28. Zickfeld, K., Slawig, T. and Rahmstorf, S.: A Reduced-Form Model for the Response of the Atlantic Thermohaline Circulation to Climate Change (2003), in press.
29. Petoukhov, V., Ganopolski, A., Brovkin, V., Claussen, M., Eliseev, A., Kubatzki, C. and Rahmstorf, S.: CLIMBER-2: A Climate System Model of Intermediate Complexity. Part I: Model Description and Performance for Present Climate. *Clim. Dyn.* 16 (2000), pp. 1–17.
30. Ganopolski, A., Petoukhov, V., Rahmstorf, S., Brovkin, V., Claussen, M., Eliseev, A. and Kubatzki, C.: CLIMBER-2: A Climate System Model of Intermediate Complexity. Part II: Model Sensitivity. *Clim. Dyn.* 17 (2001), pp. 735–751.
31. Slawig, T. and Zickfeld, K.: Parameter Optimization Using Algorithmic Differentiation in a Reduced-Form Model of the Atlantic Thermohaline Circulation (2003), submitted.
32. Mitchell, J.F.B., Johns, T.C., Eagles, M., Ingram, W.J. and Davis, R.A.: Towards the Construction of Climate Change Scenarios. *Clim. Change* 41 (1999), pp. 547–581.

33. Smith, J.B. and Pitts, G.J.: Regional Climate Change Scenarios for Vulnerability and Adaptation Assessments. *Clim. Change* 36 (1997), pp. 3–21.

34. Bruckner, T., Hooss, G., Füssel, H.M. and Hasselmann, K.: Climate System Modeling in the Framework of the Tolerable Windows Approach: the ICLIPS Climate Model. *Clim. Change* 56 (2003), pp. 119–137.

35. Hooss, G., Voss, R., Hasselmann, K., Maier-Reimer, E. and Joos, F.: A Nonlinear Impulse Response Model of the Coupled Carbon Cycle – Climate System (NICCS). *Clim. Dyn.* 18 (2001), pp. 189–202.

36. Maier-Reimer, E. and Hasselmann, K.: Transport and Storage of CO_2 in the Ocean – An Inorganic Ocean-Circulation Carbon Cycle Model. *Clim. Dyn.* 2 (1987), pp. 63–90.

37. Wigley, T.M.L.: *MAGICC (Model for the Assessment of Greenhouse-Gas Induced Climate Change): User's Guide and Scientific Reference Manual*. National Center for Atmospheric Research, Boulder, Colorado, 1994.

38. Kattenberg, A., Giorgi, F., Grassl, H., Meehl, G.A., Mitchell, J.F.B., Stouffer, R.J., Tokioka, T., Weaver, A.J. and Wigley, T.M.L.: Climate Models – Projections of Future Climate. In: J.T. Houghton, L.G. Meira Filho, B.A. Callander, N. Harris, A. Kattenberg, K. Maskell (eds.): *Climate Change 1995: The Science of Climate Change – Contribution of Working Group I to the Second Assessment Report of the IPCC*. Cambridge University Press, Cambridge, 1995, pp. 285–357.

39. Harvey, D., Gregory, J., Hoffert, M., Jain, A., Lal, M., Leemans, R., Raper, S., Wigley, T. and De Wolde, J.: *An Introduction to Simple Climate Models Used in the IPCC Second Assessment Report*. Cambridge University Press, Cambridge, 1997.

40. Houghton, J.T., Callander, B.A. and Varney, S.K. (eds.): *Climate Change 1992: The Supplementary Report to the IPCC Scientific Assessment*. Cambridge University Press, Cambridge, 1992.

41. Stouffer, R.J. and Manabe, S.: Response of a Coupled Ocean-Atmosphere Model to Increasing Atmospheric Carbon Dioxide: Sensitivity to the Rate of Increase. *J. Clim.* 12 (1999), pp. 2224–2237.

42. Schmittner, A. and Stocker, T.F.: The Stability of the Thermohaline Circulation in Global Warming Experiments. *J. Clim.* 12 (1999), pp. 1117–1133.

43. Nakićenović, N. and Swart, R.: *Emissions Scenarios*. Cambridge University Press, Cambridge, 2000.

44. Rahmstorf, S.: The Thermohaline Ocean Circulation – A System With Dangerous Thresholds? *Clim. Change* 46 (2000), pp. 247–256.

45. Cubasch, U. and Meehl, G.A.: Projections of Future Climate Change. In: J.T. Houghton, Y. Ding, D.G. Griggs, M. Noguer, P.J. van der Linden, X. Dai, K. Maskell, C.A. Johnson (eds.): *Climate Change 2001: The Scientific Basis – Contribution of Working Group I to the Third Assessment Report of the IPCC*. Cambridge University Press, Cambridge, 2001, pp. 525–582.

46. Forest, C.E., Stone, P.H., Sokolov, A.P., Allen, M.R. and Webster, M.D.: Quantifying Uncertainties in Climate System Properties With the Use of Recent Climate Observations. *Science* 295 (2002), pp. 113–117.